

Modulation of telomere terminal structure by telomerase components in *Candida albicans*

Olga Steinberg-Neifach and Neal F. Lue*

Department of Microbiology and Immunology, W. R. Hearst Microbiology Research Center, Weill Medical College of Cornell University, 1300 York Avenue, New York, NY 10021, USA

Received January 4, 2006; Revised February 7, 2006; Accepted April 18, 2006

ABSTRACT

The telomerase ribonucleoprotein in *Candida albicans* is presumed to contain at least three Est proteins: CaEst1p, CaEst2p/TERT and CaEst3p. We constructed mutants missing each of the protein subunit of telomerase and analyzed overall telomere dynamics and single-stranded telomere overhangs over the course of many generations. The *est1-ΔΔ* mutant manifested abrupt telomere loss and recovery, consistent with heightened recombination. Both the *est2-ΔΔ* and *est3-ΔΔ* mutant exhibited progressive telomere loss, followed by the gradual emergence of survivors with long telomeres. In no case was telomere loss accompanied by severe growth defects, suggesting that cells with short telomeres can continue to proliferate. Furthermore, the amount of G-strand terminal overhangs was greatly increased in the *est2-ΔΔ* mutant, but not others. Our results suggest that in addition to their well-characterized function in telomere elongation, both CaEst1p and CaEst2p mediate some aspects of telomere protection in *Candida*, with the former suppressing excessive recombination, and the latter preventing excessive C-strand degradation.

INTRODUCTION

Telomeres are nucleoprotein structures located at the ends of chromosomes that are crucial for maintaining chromosome stability (1–3). In the majority of organisms, telomeric DNA consists of short repetitive G-rich sequences that end with a single-stranded 3' overhang. In mammalian cells, the overhang can invade a more proximal region of telomeres to form a specialized D-loop, known as T-loop (4,5). Functionally important proteins are recruited to telomeres through

both DNA–protein and protein–protein interactions. Both the DNA and protein components of telomeres are essential to the maintenance of chromosome stability.

Loss of telomere DNA can occur with each round of replication due to the so-called ‘end replication problem’ (6,7). Two compensatory mechanisms that counteract telomere loss have been identified. The first entails the addition of nucleotides to the G-rich strand of telomeres by a specialized reverse transcriptase named telomerase (8–11). Telomerase is a ribonucleoprotein complex whose enzymatic core consists of a catalytic protein (named TERT in general and Est2p in yeast) and a template RNA (named TLC1 in yeast) (9). In the budding yeast *Saccharomyces cerevisiae* the telomerase complex contains at least two additional protein subunits, named Est1p and Est3p (12–14). Both subunits are required for telomere extension *in vivo*, but not essential for telomerase activity *in vitro* (9). Est1p has been subjected to detailed analysis and shown to mediate the recruitment of the telomerase complex to telomere ends by interacting with a G-strand telomere-binding protein named Cdc13p (15,16). It also appears to perform a post-recruitment or activating function (14,16). A recent study further suggests a role for the *Candida* Est1p in defining the substrate preference of telomerase *in vitro* (17). The second mechanism of telomere elongation entails recombination, and is primarily observed in telomerase-deficient cells (18–20). For example, in several budding yeasts, loss of telomerase is initially accompanied by progressive telomere shortening and senescence. However, rare populations of cells (called ‘survivors’) are able to activate a recombination-based mechanism(s) for telomere elongation and regain normal growth.

Equally important in telomere maintenance is protection of telomeric DNA from excessive nucleolytic degradation. Both single- and double-stranded telomere-binding proteins have been implicated in telomere protection. A well-studied example of single-stranded telomere-binding protein is Cdc13p in *S.cerevisiae*. Evidence for the protective function of Cdc13p came from analysis of a *cdc13^{ts}* mutant, which suffers from extensive nucleolytic degradation of

*To whom correspondence should be addressed. Tel: +1 212 746 6506; Fax: +1 212 746 8587; Email: nflue@med.cornell.edu

the C-rich strand of telomeres (21). C-strand degradation in this mutant is *EXO1*-dependent, implying a role for Cdc13p in antagonizing the activity of *EXO1* (22). A family of proteins that are similar in function to Cdc13p have been identified in diverse organisms, and are known as Pot1 (23,24). In fission yeast, loss of Pot1 function leads to telomere degradation and telomere–telomere fusion (24). In humans, RNAi-mediated knock down of Pot1 provokes changes in telomere structure and induces chromosome instability (23). Among double-stranded telomere-binding proteins, the heterodimeric Ku complex, in particular, has a well-characterized role in telomere protection. Initially identified as a key mediator of non-homologous end joining, the Ku complex was shown recently to perform multiple functions at telomeres (25,26). Like the *cdc13^{ts}* mutant, *yku* knockout strains exhibit elevated levels of G-strand overhangs at telomeres (27,28), which can also be attributed to aberrant degradation of the C-strand (22,27,28). Interestingly, several recent studies suggest that the telomerase complex, aside from its well-known function in telomere elongation, may have an additional role in telomere protection. For example, in the absence of telomerase, telomeres in the budding yeast are not only lost gradually, but also exhibit increased fusion to double-strand breaks (29). The fusion rate was even higher if the telomerase mutation was combined with the loss of Tel1p, a telomere-binding checkpoint protein. As another example, expression of telomerase mutants in human fibroblasts with shortened telomeres can prolong their life span without causing bulk telomere elongation (30).

In this study, we used *Candida albicans* as a model system for investigating telomerase function and regulation. *C.albicans* is an opportunistic fungal pathogen that can cause systemic infection in immuno-compromised individuals. It is an attractive model system because of its possession of longer telomere tracts (~2–5 Kb in the BWP17 wild-type strain), a 23 bp regular telomere repeat (31), and the availability of genome sequence. In our previous work we showed that loss of each of the individual protein component of the telomerase complex in *C.albicans* caused specific defects in telomere maintenance (32). However, we failed to observe either cell senescence, as evidenced by growth retardation, or emergence of survivors, as evidenced by improved growth and sudden telomere elongation after severe shortening. To confirm and extend these findings, we reconstructed the mutants using a different set of disruption cassettes and assessed telomere length and G- and C-strand overhangs over many more generations. Here we report that with sufficient number of passages, telomere shortening followed by the apparent emergence of survivors can be observed in the telomerase mutants, albeit without frank senescence. The *est1*- $\Delta\Delta$ mutant manifested abrupt telomere loss and recovery, consistent with heightened recombination. In addition, loss of *Est2p* was accompanied by a substantial increase in the amount of G-strand overhangs, consistent with a role for this protein in preventing aberrant degradation of the recessed C-strand. Our results suggest that in addition to their well-characterized functions in telomere elongation, both *CaEst1p* and *CaEst2p* mediate some aspects of telomere protection in *Candida*.

MATERIALS AND METHODS

Plasmids and strains

C.albicans BWP17 (*ura3*-::-*imm434/ura3*-::-*imm434 his1*::*hisG/his1*::*hisG arg4*::*hisG/arg4*::*hisG*, a gift from A. Mitchell (Columbia University)), was derived from CAI4 as described previously (33). The double knockout mutants *est1*- $\Delta\Delta$, *est2*- $\Delta\Delta$ and *est3*- $\Delta\Delta$ were created using the ‘URA-blastar’ method (34). For the disruption of *EST1*, a 426 bp fragment of the noncoding sequence upstream of the *EST1* open reading frame (ORF) was inserted 5' to the URA-blastar cassette, and a 920 bp fragment downstream of the ORF was inserted 3' to the cassette. For the disruption of *EST2*, a 768 bp fragment of the noncoding sequence upstream of the *EST2* ORF was inserted 5' to the URA-blastar cassette, and an 860 bp fragment downstream of the ORF was inserted 3' to the cassette. For the disruption of *EST3*, a 560 bp fragment of the noncoding sequence upstream of the *EST3* ORF was inserted 5' to the URA-blastar cassette, and a 980 bp fragment downstream of the ORF was inserted 3' to the cassette.

C.albicans transformations were carried out as described previously (34). Transformants were first selected on SD-Ura plates and tested for the correct integration of the URA-blastar cassette by Southern blots. *EST/est* clones that lost uracil prototrophy were selected for their ability to grow on 5-FOA plates and used for the second round of transformation with the same cassette. The loss of both alleles of *EST* genes was verified by Southern blots. All strains were grown in the YPD medium, and supplemented with 80 μ g/ml uridine when necessary.

Detection of double-stranded telomeres

For analysis of telomeres over multiple generations, cells were streaked on YPD plates, grown for 2 days at 30°C, and one colony was picked for further re-streaking and for inoculation into 5 ml YPD. The cultures were grown at 30°C and the cells collected after 16–20 h of growth. Chromosomal DNA was isolated by the ‘Smash and Grab’ method (35). The DNA (5 μ g) was digested with a combination of *AluI* and *NlaIII*. Restriction fragments were fractionated on a 0.9% agarose gel and transferred to a nylon membrane. Telomeric DNA was detected by hybridization at 65°C to a 5' end-labeled 46mer oligonucleotide containing two copies of the *C.albicans* telomere repeat. Subsequently, the nylon membrane was stripped of the telomeric probe and hybridized to a ³²P-labeled fragment of the *RAD52* gene. To compare the total telomeric DNA content in different samples, the signals from the telomeric and *RAD52* blots were quantified using a PhosphorImager system (Molecular Dynamics), and the telomeric DNA signal was normalized against the *RAD52* signal.

Plating efficiency

Colonies of the *est2*- $\Delta\Delta$ mutant at different points during the propagation were inoculated in YPD supplemented with uridine (80 μ g/ml) and grown for 16 h. Cell cultures were diluted with water and the cell densities determined using a Nuebauer hemocytometer. An aliquot containing ~300 cells was plated on a YPD plate supplemented with uridine

(80 µg/ml). Plates were incubated for 2 days at 30°C and the number of colonies counted. Plating efficiency was calculated as the ratio of the number of colonies on the plate after 2 days of incubation to the colony forming units calculated using the hemocytometer (expressed as percentages), and the results were plotted. All experiments were performed in duplicates. Note that because clumped cells were not counted, the actual number of cells used for plating was probably higher than that determined by the hemocytometer, thus resulting in plating efficiency that was higher than 100%.

In-gel hybridization assay

In-gel hybridization assays were performed as described previously with some modifications (36). Briefly, genomic DNA isolated from the wild-type and mutant *Candida* strains was digested with AluI and NlaIII, and the resulting fragments were resolved on a 0.9% agarose gel. The gel was dried on a vacuum drier for 1 h at room temperature, and subjected to pre-hybridized in the Church mix (supplemented with 100 µg/ml of boiled calf thymus DNA) for 1 h at 55°C. Hybridization was done for 3 h at 55°C using ³²P-labeled 23mer oligonucleotides complementary to either the G- or C-strand of telomeres. Subsequently, the gel was washed three times for 20 min in 4× SSC at room temperature and three times for 20 min in 4× SSC, 0.1% SDS at 55°C and exposed to a PhosphorImager screen. After an image was acquired, the gel was denatured by immersing in 0.6 M NaCl, 0.2 M NaOH for 1 h, neutralized in 1.5 M NaCl, 0.5 M Tris, pH 7.4, for 1 h, and then washed with water for 30 min. The denatured DNA in the gel was re-probed using the same oligonucleotide. The relative levels of single-stranded DNA were calculated as follows. (i) Hybridization signals for single-stranded and double-stranded telomeric DNA in each sample were quantified using a PhosphorImager system (Molecular Dynamics Inc.) and the background subtracted. (ii) The ratios for the single-stranded versus double-stranded signals were obtained for each sample. (iii) The ratios for the mutant samples were normalized against that for a wild-type sample.

Telomere oligonucleotide ligation (T-OLA) assay

The T-OLA assay was performed as described previously except for a few minor modifications (37). Briefly, 10 pmol of a 23mer oligonucleotide complementary to the G-strand or to the C-strand of telomeres (ACACCAAGAAGTTAGACATCCGT and ACGGATGTCTAACTTCTTGGTG, respectively) were 5' end-labeled using 20 U of OptiKinase (Amersham) and 10 pmol of [γ -³²P]ATP (6000 Ci/mmol, 10 mCi/ml) (Perkin Elmers) in 50 µl reaction containing 1× OptiKinase buffer (Amersham) for 30 min at 37°C, at which point 1 µl of 0.1 M cold ATP and 10 U of OptiKinase were added, followed by 15 min incubation at 37°C. Reaction was terminated by addition of 50 µl TE and phenol/chloroform extraction. Labeled oligonucleotides were purified using Nick columns (Amersham), and concentrated by ethanol precipitation and resuspension in 40 µl water. Chromosomal DNA (5 µg) was mixed with 0.5 pmol of labeled oligonucleotides in 1× *Taq* DNA ligase buffer (NEB) in 20 µl volume, and incubated at 55°C for 14–16 h. At the end of incubation, 40 U of *Taq* DNA ligase (NEB) were

added and ligation was allowed to proceed for 5 h at 55°C. Ligation was terminated by addition of 80 µl water and phenol/chloroform extraction. DNA was precipitated by the addition of ethanol and dissolved in 55 µl water. As a loading control, one-eleventh of the sample was removed for DNA quantification by electrophoresis and Ethidium Bromide staining. The remainder of the sample was dried in a vacuum dryer, dissolved in 1× sample buffer and analyzed on a 6% denaturing polyacrylamide gel. Radioactive signals were quantified using a PhosphorImager system (Molecular Dynamics), normalized against the loading control, and the relative levels of single-stranded DNA calculated as described before (38).

Slot blot

The slot/dot blot procedure was basically performed as described previously (21). Briefly, 4 µg of AluI and NlaIII-digested genomic DNA was used as the starting material. The DNA was diluted in water to a volume of 660 µl, from which a 60 µl aliquot was transferred to a fresh tube and subjected to alkali-heat denaturation (addition of NaOH to 0.2 M, followed by 30 min incubation at 65°C). Both native and denatured DNA samples were further diluted to 1200 µl in 5× SCP buffer (0.5 M NaCl, 0.15 M Na₂HPO₄ and 0.01 mM EDTA). Aliquots of DNA (300 µl per slot, four slots per sample) were applied to a Hybond-N membrane (Amersham Biosciences) by using a Microfiltration Apparatus (Bio-Rad) and immediately washed three times with equal volume of 10× SCP each. The moist membrane was exposed to UV light (Stratagene) to effect crosslinking and then divided into two equal halves. Each half of the membrane contained two slots of native and two slots of denatured DNA from each sample. Membranes were probed separately with ³²P-labeled 46mer oligonucleotides complementary to either the G- or C-strand of telomeres. Relative levels of single-stranded DNA were calculated as follows. (i) Hybridization signals for single-stranded DNA and double-stranded DNA in each sample were quantified and the background subtracted. (ii) The ratios for the single-stranded versus double-stranded signals were obtained for each sample. (iii) The ratios for the mutant samples were normalized against that for a wild-type sample.

Nuclease treatment

Chromosomal DNA was isolated by the 'Smash and Grab' method (35) and was further purified using a Nick column (Amersham). To remove the 3' single-stranded telomere overhang, ExoI (USB) was used in a reaction containing 1 U of enzyme per 50 ng of DNA in 67 mM glycine (pH 9.5), 10 mM 2-mercaptoethanol, and 6.7 mM MgCl₂, and the reaction was allowed to proceed for 24 h at 37°C. Alternatively, ExoI (Epicentre) was used in a reaction that contained 50 mM Tris-HCl (pH 7.9), 10 mM MgCl₂, 100 mM NaCl and 1 mM DTT. To remove both protruding 3' and 5' single-stranded telomere overhangs, Exonuclease VII (ExoVII, USB) was used in a reaction containing 2 U of enzyme per µg of DNA in 50 mM Tris-HCl (pH 7.9), 50 mM potassium phosphate (pH 7.6), 8.3 mM EDTA, 10 mM 2-mercaptoethanol and the reaction was performed

at 37°C for 30 min. Reactions were terminated by phenol/chloroform extraction and processed for subsequent assays.

RESULTS

Construction of the *C.albicans est* mutants

Previously, we reported results of a study in which the telomere dynamics of *C.albicans* mutants was followed through ~250–300 generations (32). Though some defects in telomere maintenance were observed, we failed to detect senescence or the emergence of survivors, as judged by changes in the growth rate of cultures. To explore the possibility that more extended passaging of the mutants may reveal additional phenotypes, we reconstructed the mutants, propagated them for ~800 generations, and analyzed telomere lengths and structure during the passages. For the current study we deleted the *EST* genes using the ‘URA-blasters’ method. In comparison with the ‘One-Step Transformation’ method used in the earlier study, the ‘URA-blasters’ technique has the advantage of precluding the homozygosis of genes located distal to the disrupted gene (32,39). Transformation cassettes in the current study were created by inserting short DNA fragments that flank the ORF of the target gene upstream and downstream of the ‘URA-blasters’ cassette (Materials and Methods). Double deletion mutants were derived from two rounds of transformation and selection and confirmed by Southern blots (data not shown). The mutants were propagated by re-streaking every 2 days for isolated colonies. It is estimated that each restreak corresponds to ~25 generations of growth.

Growth and telomere dynamics of the *est* mutants during extended passage

We next investigated the overall telomere dynamics of the wild type and mutants during extended passage. For the wild-type parental strain used in this study (BWP17), the majority of *Nla*III and *Alu*I digested telomere restriction fragments are between 2 and 5 kb in size. Consistent with the earlier report, we found that the size of telomere fragments and their distribution in the wild-type strain differed from one streak to the next (Figure 1A). However, the variations between the total intensity of the telomeric signals over time are no more than 20%. We have passaged the BWP17 for a total of 25 streaks without observing noticeable changes in telomeric content (data not shown). These data are in agreement with our earlier observation that some changes in telomere length occur normally during the propagation of *C.albicans* cells, but a homeostatic mechanism must be acting to maintain the telomeric content of the cell within a range.

For analysis of mutants, we examined the telomere dynamics of two or three clones (three for *est2*- $\Delta\Delta$ and two each for *est1*- $\Delta\Delta$ and *est3*- $\Delta\Delta$) for each telomerase mutant, which yielded similar results. The newly derived *est1*- $\Delta\Delta$ strains were passaged for >30 restreaks after the selection of the mutant (Figure 1B). Significant telomere loss was observed during passage, with the total telomere content showing an almost 50% decrease at streak 11 (data not shown). However, large telomeric fragments were still

present at streak 17. Presence of long telomeres in combination with overall telomere loss in the *est1*- $\Delta\Delta$ strain suggests that telomeres in the mutant were more heterogeneous in size than the wild type. Long telomeres became absent for several passages (streak 19–25) but reappeared thereafter. This was accompanied by restoration of telomere content to wild-type levels. Such an abrupt increase of telomere length *en masse* is reminiscent of type II survivors that arose after senescence in telomerase-negative *S.cerevisiae* strains. We have thus adopted the name ‘survivors’ to describe the *Candida* cells, notwithstanding some phenotypic differences between the *Saccharomyces* and *Candida est1* mutant. Most notably, in the *C.albicans est1*- $\Delta\Delta$ clone there was no decrease in the growth rate during passage (data not shown), and the telomere content of the mutant never fell below 20% of the wild type. Even in the population with the shortest average telomere length, it was possible to detect telomeric restriction fragments that were at least 2 kb long. After the emergence of ‘survivors’, telomere content of the *est1*- $\Delta\Delta$ clone became comparable with that of the wild type and was maintained during the remaining passages. It is unclear if additional cycles of telomere loss and restoration can occur in these cells with even more extended subculturing.

In contrast to *Est1p*, loss of *Candida Est2p* resulted in progressive telomere attrition (Figure 1C). Notably, while occasional lengthening and shortening events were observed in the *est2*- $\Delta\Delta$ mutant, they were not as frequent as in the case of *est1*- $\Delta\Delta$ mutant (compare Figure 1B and C, see also Supplementary Figure 1), nor did telomere length distribution in any *est2*- $\Delta\Delta$ clone become as heterogeneous as *est1*- $\Delta\Delta$. All telomeres became shorter than 1 kb at about the 19th streak, but subsequently underwent significant elongation, which was followed by a second round of contraction. This dynamics, which is similar to that of *S.cerevisiae* telomerase mutants, was not observed in the previous study of another *Candida est2*- $\Delta\Delta$ mutant, most likely due to the shorter duration of the earlier experiment (32). It is also possible that the earlier mutant may have suffered some additional genetic changes due to the ‘UAU1’ knockout protocol. The greater reliability of the URA-blasters transformation protocol and the more extended passaging of the mutant suggest that the current results are more reflective of the true consequences of deleting *EST2* in *Candida*. Like the *Candida est1*- $\Delta\Delta$ mutant, the *est2*- $\Delta\Delta$ ‘survivors’ exhibited features that were distinct from their *S.cerevisiae* counterparts. First, loss of *Est2p* functions in *C.albicans* did not result in severe growth defects even after prolonged propagation. Mild growth retardation was detected in the *est2*- $\Delta\Delta$ strain in liquid media (Figure 2A). However, this was true for cultures of early and late passages, and does not appear to be due primarily to telomere attrition. From the exponential phase of the growth curves, it was estimated that the doubling time of the mutant was increased by ~20%. Growth of *est2*- $\Delta\Delta$ was further investigated by measurement of plating efficiency. As shown in Figure 2B, the plating efficiency of the mutant was slightly reduced (by ~20%) when monitored at three different points during passage. Thus, the growth retardation of *est2*- $\Delta\Delta$ may be due to loss of viability of a small fraction of the cells. Another distinct feature of *C.albicans est2*- $\Delta\Delta$ mutant relates to the kinetics of telomere

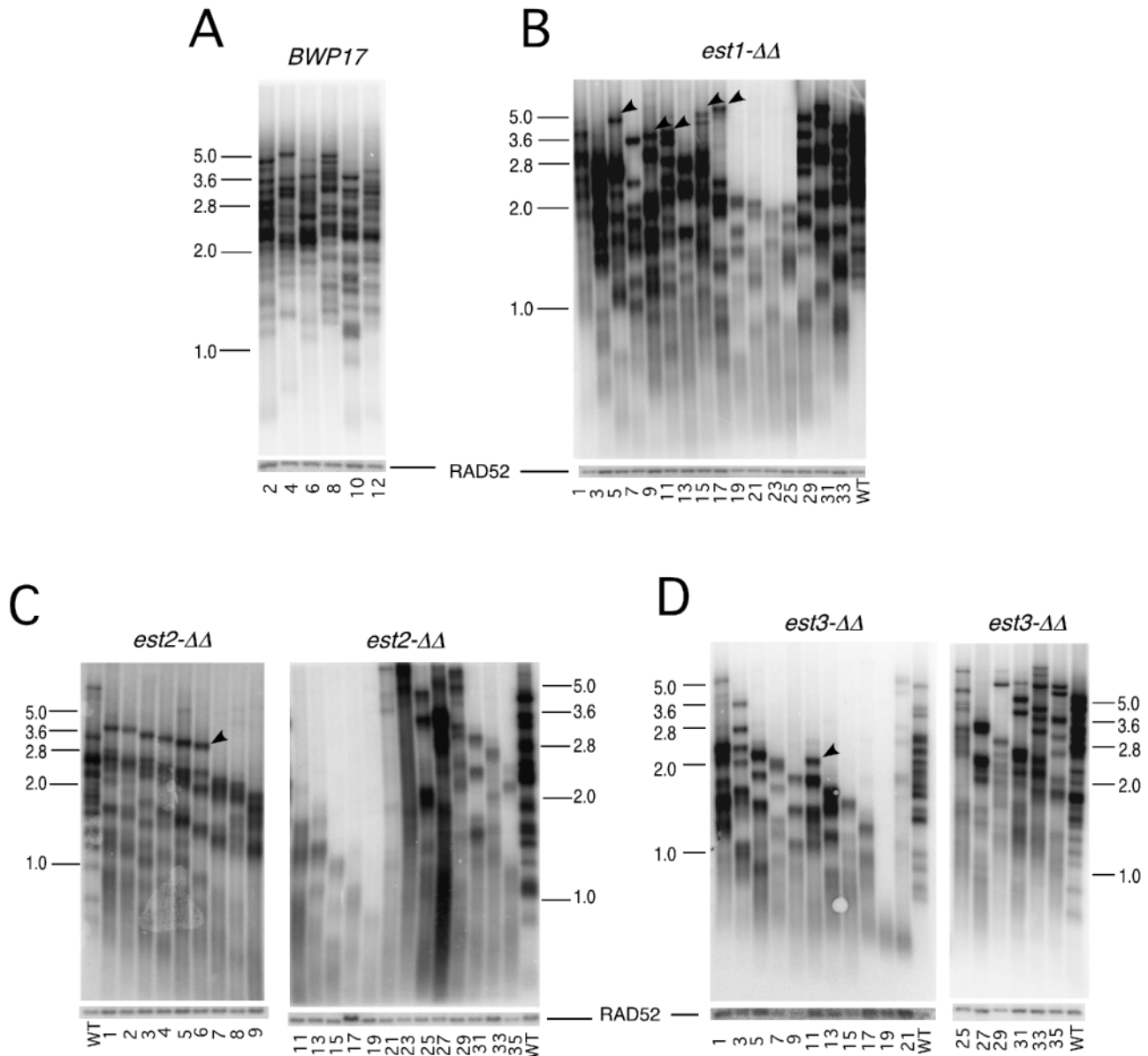


Figure 1. Telomere dynamics in the wild-type and *est* mutant strains. Telomeres dynamics was analyzed in successive generations of the wild-type and the *est* mutant strains by Southern blots. The blots were stripped and re-probed using a labeled *RAD52* fragment and the results shown at the bottom. The strains and passages analyzed are (A) BWP17, streaks 2–12; (B) *est1-ΔΔ*, streaks 1–33; (C) *est2-ΔΔ*, streaks 1–35; (D) *est3-ΔΔ*, streaks 1–35. Instances of sudden appearance and disappearance of telomere restriction fragments are marked by arrows.

elongation in the cell population. At streak 21, there was an abrupt broadening in the length distribution of telomeres, indicating that the population of cells contained both very long and short telomeres. Whether the long and short telomeres co-exist in a single cell is unclear. Over the next few streaks the relative intensity of the long telomeres increased steadily and became dominant. These observations suggest that cells with shortened telomeres in the *est2-ΔΔ* mutant culture were able to proliferate and co-exist with apparent ‘survivors’. Lastly, the telomere lengths of *Candida est2-ΔΔ* survivors are comparable with those of wild-type cells, whereas the *Saccharomyces* type II survivors have telomeres that are dramatically longer than normal. Thus, as in the case of *est1* mutants, there are apparent similarities

as well as significant differences between the *Candida* and *S.cerevisiae est2* survivors.

Telomeres in the new *est3-ΔΔ* mutants experienced progressive loss (Figure 1D), just as described for the previous *est3-ΔΔ* mutant (32). Similar to *est1-ΔΔ* and in contrast to *est2-ΔΔ*, no growth retardation was evident during passage of the *est3-ΔΔ* mutant (data not shown). At streak 21, after severe telomere attrition, there was an abrupt appearance of long telomeres, which became pre-dominant during the later streaks. Interestingly, unlike the *est2-ΔΔ* strain, bulk telomere content after recovery was preserved in 1 *est3-ΔΔ* survivor for ~10 streaks (Figure 1D), suggesting potential variability in the dynamics of the survivors. Analysis of more clones will be necessary to confirm the prevalence

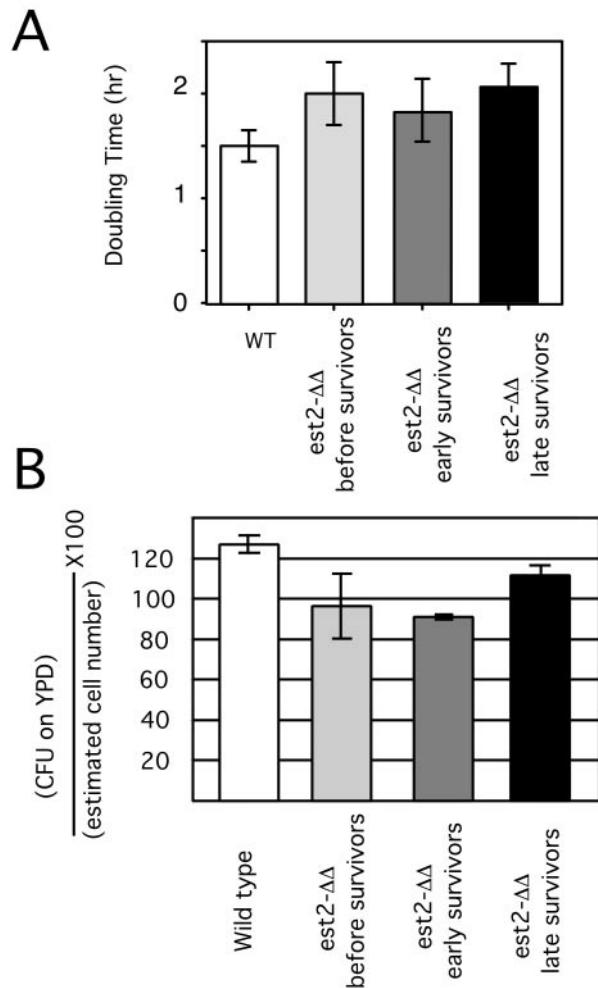


Figure 2. Growth of the *est2-ΔΔ* mutant. (A) The doubling time for the wild-type and *est2-ΔΔ* strain during exponential growth was determined at three different points during passage and plotted. (B) The plating efficiency of the wild-type and *est2-ΔΔ* strain during passage was determined as described in Materials and Methods and plotted.

of this variability. We conclude that telomere attrition followed by the apparent emergence of survivors can be observed in *Candida* following prolonged passage of telomerase-deficient clones.

Detection of G- and C-strand overhangs at *Candida* telomeres using in-gel hybridization

It has been suggested that telomerase may have a protective function that is independent of its telomere extension function. Loss of telomere protection has been linked to changes in the level of terminal overhangs. We therefore investigated the impact of *Candida* telomerase mutations on the amount of telomere overhangs. Several methods have been developed previously for the purpose of quantifying single-stranded telomere overhangs (21,37,39). For analysis of *Candida* telomeres, we adopted in-gel hybridization as our primary assay because this technique has been used widely by many laboratories to analyze telomeres in different organisms. As described later, we also confirmed the

key conclusions of the in-gel analysis using two additional assays.

We first investigated samples of chromosomal DNA from BWP17 using in-gel hybridization, and found that low levels of G- and C-strand signals could be detected at telomeres (Figures 3 and 4 and data not shown). The G-strand signal was abolished by pre-treatment of DNA with ExoI, a single-stranded 3'→5' exonuclease (Figure 3A, lanes 3 and 4). In contrast, the bulk telomere signals obtained after denaturation of the DNA were unaffected by this treatment (Figure 3A, lanes 5 and 6). Both the G-strand and C-strand signals for native DNAs were also sensitive to ExoVII, a single-strand specific 3'→5' and 5'→3' exonuclease (Figure 3B and data not shown). These results indicate that most of the native in-gel signals were due to terminal overhangs. We note that the native in-gel signals were generally less discreet in size than the signals obtained after denaturation and re-probing. One potential explanation is that DNA fragments with significant overhangs may represent a small fraction of the telomere restriction fragments, and may behave more heterogeneously due to variable amount of single-stranded overhangs. The native and denatured signals, however, do exhibit similar size distributions in a given sample, consistent with their similar origins (Figures 3 and 4).

G- and C-strand overhangs in *est* mutants

Chromosomal DNAs derived from *Candida est* mutants were first subjected to in-gel hybridization analysis using a probe complementary to the G-strand. For each mutant, we investigated two independent clones over ~10 successive streaks. Remarkably, loss of Est2p had a strong impact on the level of unpaired G-strand: there was an up to 20-fold increase in the amount of G-strand overhangs during passage, when the G-strand signals were normalized against total telomeric DNA (Figure 4A). The increase was observed in both mutant clones and in multiple samples, and the signals were sensitive to ExoI and ExoVII treatment (Supplementary Figure 2). These results suggest that loss of *Candida* Est2p may result in aberrant degradation of the 5' end-containing C-strand, thus leading to the accumulation of unpaired G-strand. Comparison of the signals in native and denatured gel images indicates that within a given sample, shorter DNA fragments possess higher levels of G-strand overhangs than longer fragments. For example, the "*" sample yielded two major peaks in both the native and denatured analysis (~3.6 and 2.3 kb, Figure 4A and C). The signal for the lower peak was stronger in the native analysis, but weaker in the denatured analysis (Figure 4C, left). Likewise, the lower peak in the "*" sample was comparable in intensity to the upper peak in the native analysis, but much weaker in the denatured analysis (Figure 4C, right). Quantitative analysis of other samples yielded similar results (data not shown). Thus, shorter telomeres appear to be more susceptible to C-strand degradation in the *est2-ΔΔ* mutant. In contrast to *est2-ΔΔ*, the amount of G-strand overhang in the *est1-ΔΔ* and *est3-ΔΔ* mutant were quite low and indistinguishable from that found in the parental strain (Figure 5A and B).

Unpaired C-strand in the *est* mutants was also investigated by in-gel hybridization using a probe that corresponds to the G-strand repeat. Again, loss of Est2p had the most impact on

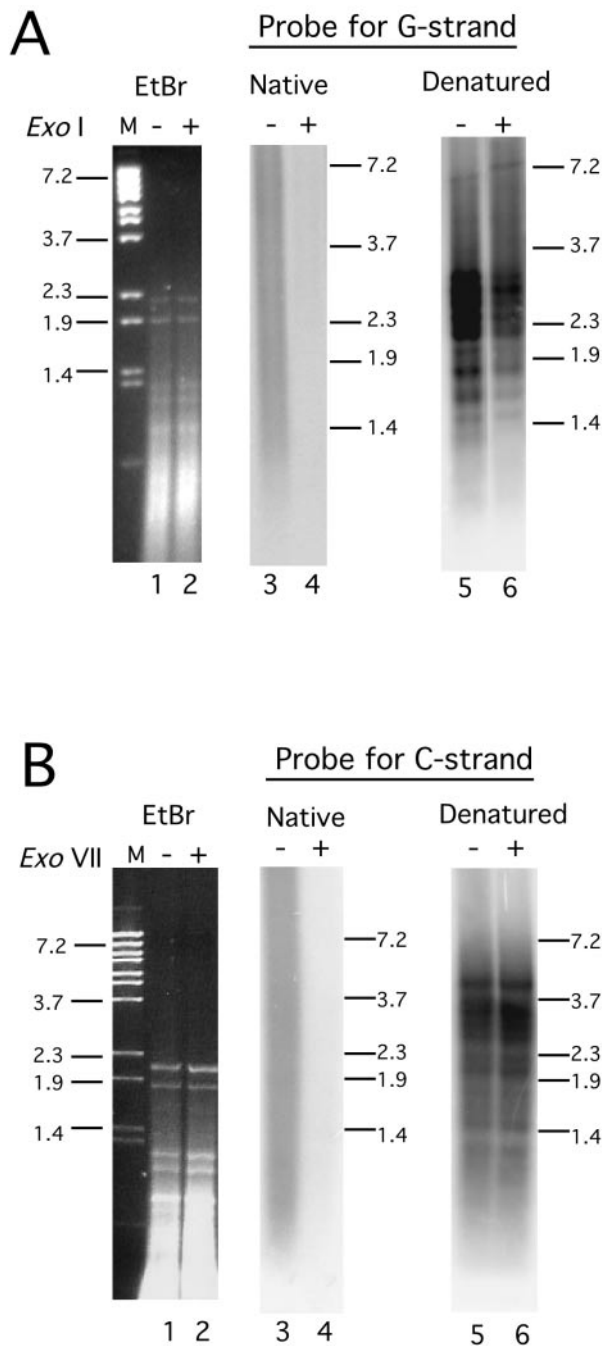


Figure 3. The effect of nuclease treatment on the amount of unpaired telomeric overhangs. (A) DNA isolated from BWP17 was incubated with or without *E.coli* ExoI, and then treated with AluI and NlaIII. The resulting samples were first analyzed by gel electrophoresis and ethidium bromide staining (left panel). The gel was subsequently dried and subjected to in-gel hybridization using a probe complementary to the G-strand of *Candida* telomere repeat (middle panel). The DNA in the gel was then denatured and hybridized again to the same probe (right panel). (B) DNA isolated from BWP17 was incubated with or without *E.coli* ExoVII, and then treated with AluI and NlaIII. The resulting samples were first analyzed by gel electrophoresis and ethidium bromide staining (left panel). The gel was subsequently dried and subjected to in-gel hybridization using a probe complementary to the C-strand of *Candida* telomere repeat (middle panel). The DNA in the gel was then denatured and hybridized again to the same probe (right panel).

the amount of unpaired C-strand (Figure 4C). There was a moderate decrease ($\sim 40\text{--}70\%$) in the amount of C-strand overhang in the two clones of *est2*- $\Delta\Delta$ mutant during the course of 10 streaks. In contrast to *est2*- $\Delta\Delta$, the amount of C-strand overhangs in the *est1*- $\Delta\Delta$ and *est3*- $\Delta\Delta$ mutant was similar to that found in the parental strain (data not shown). Thus, loss of individual subunits of the *Candida* telomerase complex has different impacts on the telomere overhang structure.

Analysis of telomere overhangs by the T-OLA and slot blot assay

Because changes in telomere overhangs have not been observed in pre-senescent telomerase mutants before, we sought to verify our in-gel hybridization results for *est2*- $\Delta\Delta$ using two other assays, namely the slot blot and T-OLA assay (21,36,37). These assays detect single-stranded telomere overhangs by hybridizing native DNAs on nylon membranes and in solution, respectively, to strand-specific probes. In the case of T-OLA, multiple copies of the probe that annealed to the single-stranded overhangs are further ligated and subsequently analyzed by gel electrophoresis. Chromosomal DNAs derived from wild-type and *est2*- $\Delta\Delta$ mutant were subjected to both assays. As shown in Figures 6 and 7, the *est2*- $\Delta\Delta$ mutant consistently displayed higher levels of G-strand signals in comparison with the wild-type samples in both T-OLA and slot blot assays. The average increases were $\sim 7\text{-}$ and 10- fold in the T-OLA and slot blot assays, respectively (Figures 6B and 7). In contrast, the C-strand signals yielded by the mutant samples were somewhat lower than the wild type (Figure 7 and data not shown). These findings are entirely consistent with the results of the in-gel hybridization analysis. Thus, alterations in the amount of telomere overhangs in the *est2*- $\Delta\Delta$ mutant can be detected by three different assays.

Accumulation of G-strand overhangs in the *est2*- $\Delta\Delta$ clones was due to the loss of Est2p

Even though we observed accumulation of unpaired G-strand in several independent *est2*- $\Delta\Delta$ clones, it remains formally possible that this phenotype was due to unrelated genetic changes that occurred during the multiple steps required for mutant strain derivation. To definitively rule out this possibility, we re-integrated one wild-type copy of the *EST2* gene at a disrupted locus, and analyzed the phenotypes of the resulting strain. Telomere length measurements through successive streaks indicate that the strain is capable of maintaining telomere lengths over many generations (data not shown). Importantly, the level of G-strand overhangs in the re-integrand is comparable with the wild-type strain and much lower than the *est2*- $\Delta\Delta$ mutant from which the re-integrand was derived (Figure 8A and C). As expected, the overall telomeric content of the re-integrand was higher than the *est2*- $\Delta\Delta$ mutant (Figure 8B). We conclude that the accumulation of G-strand overhangs in the *est2*- $\Delta\Delta$ mutant must be due to the loss of Est2p rather than some other unintended genetic changes.

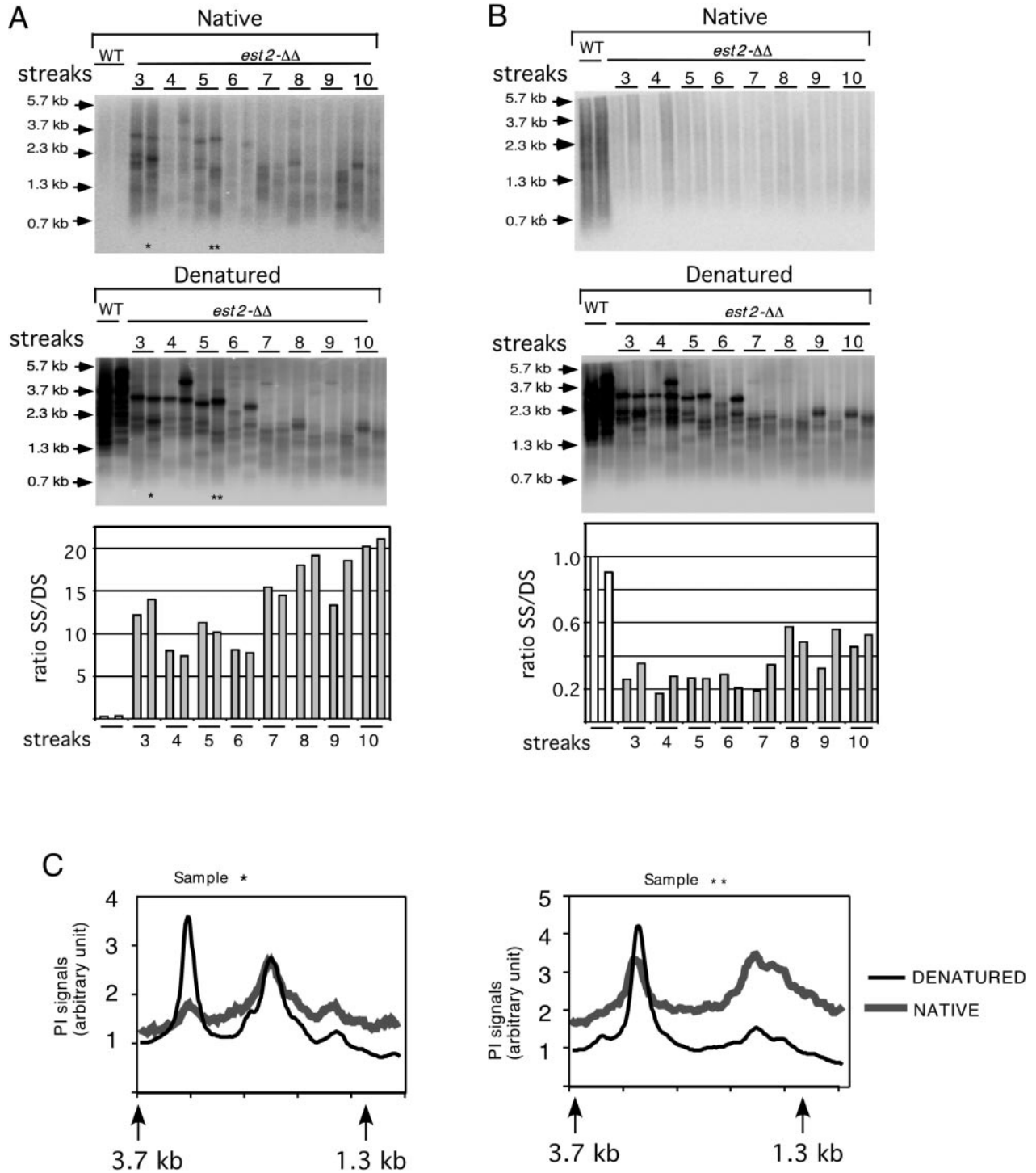


Figure 4. Analysis of G-strand overhangs in the wild-type and *est2-ΔΔ* mutant clones. (A) (Upper panel) Genomic DNA was isolated from overnight cultures of the wild-type strain and the indicated streaks of the *est2-ΔΔ* mutant, and subjected to in-gel hybridization analysis using an oligonucleotide probe complementary to the G-strand of *Candida* telomeres. (Middle panel) After probing the native DNA with strand-specific probes, the DNA in the gel was denatured and hybridized again with the same probe. (Lower panel) The hybridization signals for single- and double-stranded telomeres were quantified, and the ratios plotted. (B) Same as (A) except that the probe was designed to anneal to the C-strand of *Candida* telomeres. (C) The intensity traces for the lanes labeled '*' and '**' in Figure 4A were obtained using the Imagequant program (Molecular Dynamics Inc.). The native and denatured profiles for each sample are plotted alongside each other.

DISCUSSION

In this study, we investigated the total amount and length of telomeric DNA in *Candida* mutants that are missing

individual components of the telomerase complex during extended passage. In addition, we analyzed the levels of single-stranded telomere overhangs in the same strains. Significant findings include (i) apparent observation of

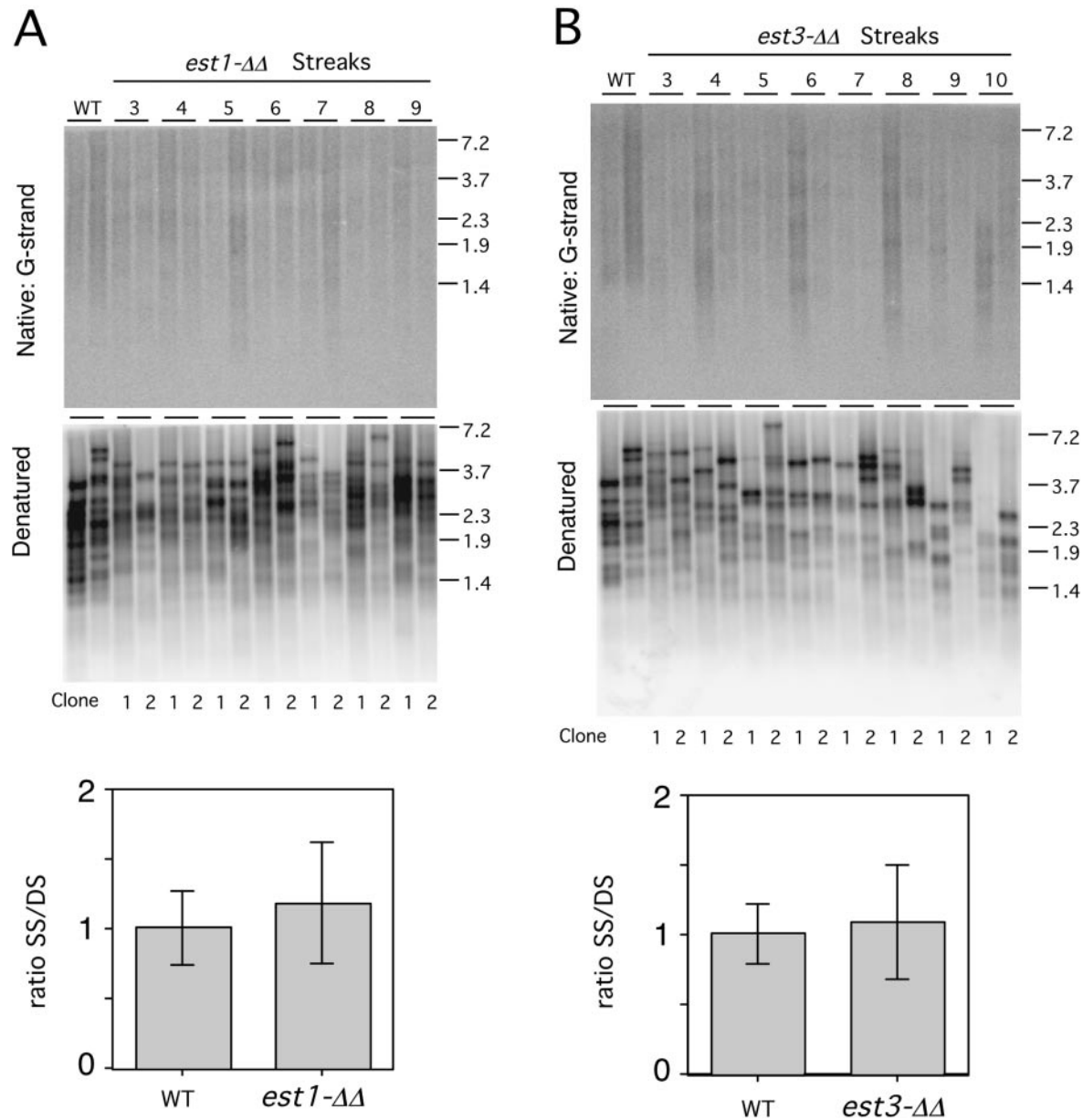


Figure 5. Analysis of G-strand overhangs in the *est1-ΔΔ* and *est3-ΔΔ* mutant clones. (A and B) (Upper panel) Genomic DNA was isolated from overnight cultures of the wild-type strain and the indicated streaks of the *est1-ΔΔ* or *est3-ΔΔ* mutant, and subjected to in-gel hybridization analysis using an oligonucleotide probe complementary to the G-strand of *Candida* telomeres. (Middle panel) After annealing the native DNA with the G-strand-specific probe, the DNA in the gel was denatured and hybridized again with the same probe. (Lower panel) The ratios of G-strand signals to double-stranded telomere signals were calculated for both the wild-type and mutant samples and the averages and standard deviations plotted.

telomerase-deficient survivors, (ii) increased levels of telomere recombination in the *est1-ΔΔ* mutant, (iii) accumulation of G-strand overhangs in the *est2-ΔΔ* mutant, and (iv) detection of C-strand overhangs. We also compared three different methods for assessing telomere overhangs and found that they yielded qualitatively similar results.

Telomerase-deficient *C.albicans* survivors

In our earlier analysis of *Candida* telomerase mutants, we did not observe the emergence of survivors (32), most likely due to insufficient number of passages. Here we show that with

extended subculturing, phenotypes that are reminiscent of *S.cerevisiae* survivors can indeed be observed in *Candida* mutants. Specifically, both the *est2-ΔΔ* and *est3-ΔΔ* strains suffered progressive telomere attrition, followed by the emergence of survivors with greatly elongated telomeres. Some interesting differences, however, can be noted between the *S.cerevisiae* and *Candida* survivors. In *S.cerevisiae*, survivors do not arise until the culture has suffered very significant growth defects. The appearance of survivors is correlated with the detection of longer than wild-type telomeres in the vast majority of cells and is accompanied by an increase in the growth rate of the culture (19,40–42).

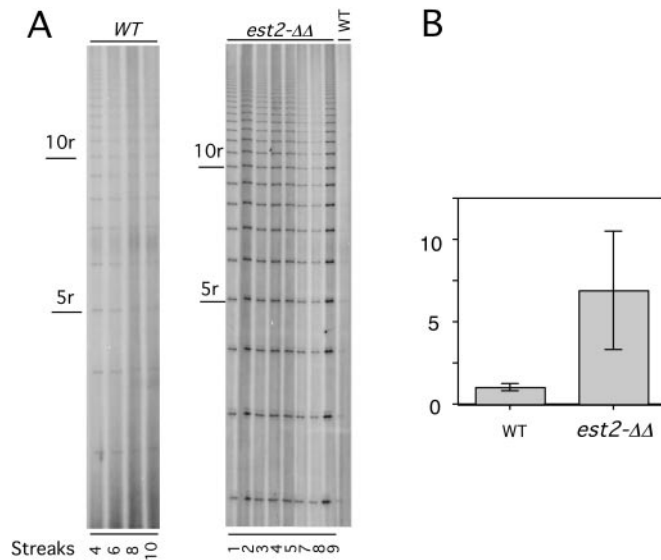


Figure 6. T-OLA analysis of unpaired G-strand overhangs in the wild-type and *est2-ΔΔ* strains. (A) G-strand overhang dynamics was analyzed in successive generations of the wild type and the *est2-ΔΔ* mutant strain by T-OLA. Selected T-OLA products are designated by the number of repeats that they contain. The strains and passages analyzed in the different parts of the figure are BWP17, streaks 4–10; *est2-ΔΔ*, streaks 1–9. (B) The relative levels of G-strand overhangs were quantified for the wild-type (streaks 4, 6, 8 and 10) and *est2-ΔΔ* samples (streaks 1–9) as described in Materials and Methods, and the averages and deviations plotted.

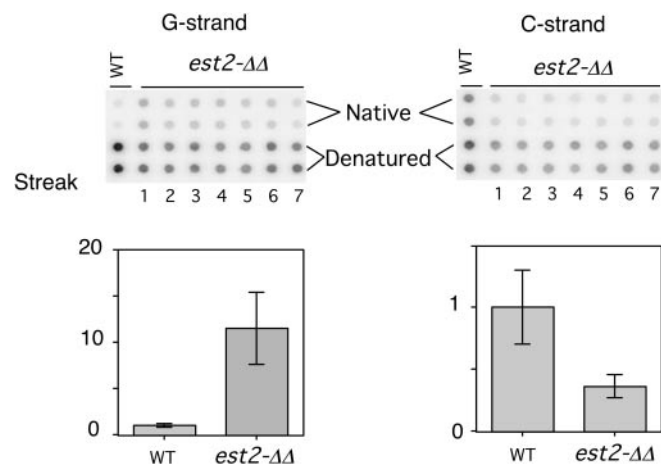


Figure 7. Slot blot analysis of unpaired G- and C-strand overhangs in *est2-ΔΔ* mutant. Genomic DNA was isolated from overnight cultures of the wild-type strain and the indicated streaks of the *est2-ΔΔ* mutant, and subjected to slot blot analysis. Note that 10 times more native DNA than denatured DNA was applied to the slots in order to generate appreciable signals in these analyses (Materials and Methods). In all cases analyzed, the denatured DNA yielded a signal that is at least 30 times stronger than the native DNA when corrected for this difference in application. Relative ratios of single-stranded to double-stranded telomere DNA for wild-type (duplicate samples for streak 2) and *est2-ΔΔ* (streaks 1–7) in the slot blots were calculated (Materials and Methods) and plotted at the bottom.

In *C.albicans*, the emergence of survivors does not coincide with a large change in the growth rate of the culture. Thus, either telomere attrition has little effect on *C.albicans* growth, or the activation of the recombination pathway occurs before the degree of telomere attrition that is necessary to

induce large growth defects. Also in contrast to *S.cerevisiae*, the *Candida* survivors initially have telomeres that are comparable in lengths with the wild type. The formation and behavior of *Candida* survivors appear to resemble more closely those of another budding yeast *Kluyveromyces lactis*, where senescence can also be accompanied by relatively mild growth defects (43). Indeed, a recent study of *K.lactis* telomeres demonstrates that senescence in telomerase-deficient cells can be suppressed by the introduction of a single elongated telomere (44). Given the greater heterogeneity of *Candida* telomere length distribution, the possibility that a few long telomeres might be stochastically present in telomerase-negative mutants even after prolonged passage to suppress senescence must also be considered. One potentially important distinction between the current analysis and previous studies of other budding yeasts is that all of our work was performed using diploid cells, whereas almost all of the published work on *S.cerevisiae* and *K.lactis* was done using haploid yeast. It remains to be seen if any of the distinct features of *Candida* with regard to telomere maintenance can be attributed primarily to its diploid nature.

Heightened telomere recombination in the *Candida est1-ΔΔ* mutant

The telomere dynamics of the *C.albicans est1-ΔΔ* mutant differs substantially from that of the other mutants and its *S.cerevisiae* counterpart (40,45). Long telomeres can persist upon extended subculturing, and there are instances of sudden telomere loss and acquisition (Figure 2B). While instances of sudden telomere loss and acquisition were also observed in *est2-ΔΔ* and *est3-ΔΔ* mutants, they were not as frequent, and telomeres in these mutants never reached the level of heterogeneity seen in *est1-ΔΔ* before the emergence of survivors. These results suggest that in *est1-ΔΔ* recombinational elongation of relatively long telomeres occurs at somewhat higher frequencies than in other mutants. This hypothesis can explain the absence of severe telomere shortening in early generations, and the maintenance of telomere content at the wild-type levels in later generations. It is tempting to speculate that loss of Est1p may increase the accessibility of telomeres to recombination proteins. In other words, Est1p appears to ‘protect’ telomeres against recombination that otherwise can occur only on severely shortened telomeres (46). A protective function for Est1 at telomeres was also suggested by recent analyses of the human and *Schizosaccharomyces pombe* homologs (47,48).

If the dynamics of telomeres in *est1-ΔΔ* were due to heightened recombination, then it ought to be dependent upon recombination proteins. Several attempts were made to generate an *est1-ΔΔ rad52-ΔΔ* mutant without success. Because unlike *S.cerevisiae*, loss of Rad52p alone in *Candida* causes severe growth defects (49), it is unclear whether our failure was due to this growth defect or possibly a synthetic interaction between telomerase and *RAD52* in *Candida*. Additional studies are underway to address this issue.

Prevention of aberrant C-strand resection by *Candida Est2p*

Perhaps the most interesting finding from our investigation of telomere overhangs is the substantial buildup of such overhangs in the *est2-ΔΔ* mutant. This buildup can be seen even

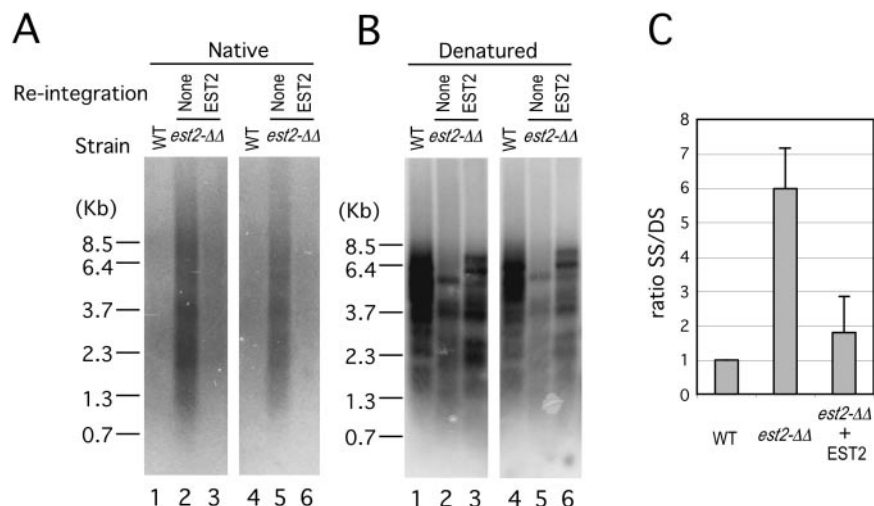


Figure 8. Analysis of G-strand overhangs in wild type, *est2-ΔΔ* and *est2-ΔΔ* with a re-integrated copy of *EST2*. (A) Genomic DNA was isolated from overnight cultures of a wild-type strain, an *est2-ΔΔ* mutant, and an *est2-ΔΔ* mutant with a re-integrated copy of *EST2*, and subjected to in-gel hybridization analysis using an oligonucleotide probe complementary to the G-strand of *Candida* telomeres. Lanes 1–3 and 4–6 represent duplicate assays of the same samples. (B) After probing the native DNA with strand-specific probes, the DNA in the gel was denatured and hybridized again with the same probe. (C) Relative ratios of single-stranded to double-stranded telomere signals for all three samples were calculated and plotted.

in early generations of the mutant. While accumulation of unpaired G-strand has been reported previously for an *S.cerevisiae est1-Δ* mutant, the accumulation was only observed after severe telomere attrition and is likely to be mechanistically distinct (50). Study of *S.cerevisiae yku* and *cdc13* mutants demonstrates that abnormally long G-strand is created through resection of the C-strand, at least in part by the *EXO1* nuclease (22,50,51). That this phenotype is observed with the loss of Est2p (but not Est1p or Est3p) in *C.albicans* suggests that Est2p may have a similar role in protecting telomeres against excessive nucleolytic degradation. The apparently increased sensitivity of short telomeres to C-strand degradation suggests that the protective function of Est2p may be more important for short telomeres. Why should the Est2p component of telomerase alone possess this unique activity? One speculative explanation can be proposed based on earlier findings in *S.cerevisiae*. In *S.cerevisiae*, Est2p is localized to telomeres throughout the cell cycle, at least in part through an indirect association with the Ku complex (i.e. Est2p binds telomerase RNA, which in turn binds Ku) (52–54). The Est2p–Ku interaction may thus enhance the ability of the entire complex to prevent nuclease attack. In contrast, there is no evidence that the association of Est1p and Est3p with telomeres is stable throughout the cell cycle (16). Because telomerase RNA is also presumed to be part of the protective complex, it is tempting to speculate that deleting the RNA gene may also cause accumulation of G-strand overhangs. Further studies will be necessary to determine the validity of this hypothesis.

C-strand overhangs in *C.albicans*

Presence of C-strand overhangs has only been described previously for human telomeres using the T-OLA assay (55), and not for any fungi. Our detection of such overhangs in *C.albicans* is therefore unexpected. Nevertheless, the biology of *C.albicans* (e.g. the obligate diploid genome) is

sufficiently distinct from *S.cerevisiae* to make such differences in telomere structure far from implausible. The most obvious change in the *Candida* C-strand overhangs associated with telomerase mutations was a moderate decrease observed in the *est2-ΔΔ* samples. The functional significance of this finding is unclear. It is worth noting that because the wild-type samples yielded stronger signals for both single-stranded and double-stranded telomeres, if the hybridization signals are not strictly linear with respect to the levels of single and double-stranded DNA, then the quantitative differences we calculated may be more apparent than real. Additional studies are necessary to address this possibility. (On the other hand, our conclusion with respect to G-strand alterations in the *est2-ΔΔ* mutant is not subject to the same caveat, because the mutant samples consistently yielded weaker signals for double-stranded telomeres, but stronger signals for single-stranded telomeres.)

CONCLUSIONS

Altogether, our analysis of the telomere length dynamics and G-strand variations in the mutant strains support a role for both *Candida* Est1p and Est2p in telomere protection. In the case of *est1-ΔΔ*, loss of protection is mainly manifested as heightened recombination at telomeres. In the case of *est2-ΔΔ*, loss of protection is mainly manifested as accumulation of G-strand overhangs. That the phenotypic consequences are different for the two mutants implies that the precise mechanisms of protection must also be different.

SUPPLEMENTARY DATA

Supplementary Data are available at NAR Online.

ACKNOWLEDGEMENTS

We are grateful to Dr Shu-Chun Teng for constructive comments on the manuscript. We also thank Sunitha Singh and You-Chin Lin for help with the construction of mutant strains, Alain Dandjinou for help with in-gel hybridization, and Drs E. D'Ambrosio, S. Stewart and I. Ben-Porath for advice on T-OLA. This work was supported by a New Investigator Award in Pathogenic Mycology from Burroughs Wellcome Fund and a grant from NIH. Funding to pay the Open Access publication charges for this article was provided by the Irma Hirschl Monique Weill-Caulier Trust.

Conflict of interest statement. None declared.

REFERENCES

- Blackburn,E. (2001) Switching and signaling at the telomere. *Cell*, **106**, 661–673.
- Ferreira,M., Miller,K. and Cooper,J. (2004) Indecent exposure: when telomeres become uncapped. *Mol. Cell*, **13**, 7–18.
- Cech,T. (2004) Beginning to understand the end of the chromosome. *Cell*, **116**, 273–279.
- Griffith,J.D., Comeau,L., Rosenfield,S., Stansel,R.M., Bianchi,A., Moss,H. and de Lange,T. (1999) Mammalian telomeres end in a large duplex loop. *Cell*, **97**, 503–514.
- de Lange,T. (2002) Protection of mammalian telomeres. *Oncogene*, **21**, 532–540.
- Olovnikov,A. (1973) A theory of marginotomy. The incomplete copying of template margin in enzymic synthesis of polynucleotides and biological significance of the phenomenon. *J. Theor. Biol.*, **41**, 181–190.
- Lingner,J., Cooper,J. and Cech,T. (1995) Telomerase and DNA end replication: no longer a lagging strand problem? *Science*, **269**, 1533–1534.
- Greider,C.W. and Blackburn,E.H. (1985) Identification of a specific telomere terminal transferase activity in Tetrahymena extracts. *Cell*, **43**, 405–413.
- Nugent,C.I. and Lundblad,V. (1998) The telomerase reverse transcriptase: components and regulation. *Genes Dev.*, **12**, 1073–1085.
- Kelleher,C., Teixeira,M., Forstemann,K. and Lingner,J. (2002) Telomerase: biochemical considerations for enzyme and substrate. *Trends Biochem. Sci.*, **27**, 572–579.
- Harrington,L. (2003) Biochemical aspects of telomerase function. *Cancer Lett.*, **194**, 139–154.
- Lundblad,V. (2003) Telomere replication: an Est fest. *Curr. Biol.*, **13**, R439–R441.
- Hughes,T.R., Evans,S.K., Weilbaecher,R.G. and Lundblad,V. (2000) The Est3 protein is a subunit of yeast telomerase. *Curr. Biol.*, **10**, 809–812.
- Evans,S. and Lundblad,V. (2002) The Est1 subunit of *Saccharomyces cerevisiae* telomerase makes multiple contributions to telomere length maintenance. *Genetics*, **162**, 1101–1115.
- Pennock,E., Buckley,K. and Lundblad,V. (2001) Cdc13 delivers separate complexes to the telomere for end protection and replication. *Cell*, **104**, 387–396.
- Taggart,A., Teng,S. and Zakian,V. (2002) Est1p as a cell cycle-regulated activator of telomere-bound telomerase. *Science*, **297**, 1023–1026.
- Singh,S. and Lue,N. (2003) Ever shorter telomere 1(EST1)-dependent reverse transcription by *Candida* telomerase *in vitro*: evidence in support of an activating function. *Proc. Natl Acad. Sci. USA*, **100**, 5718–5723.
- Neumann,A. and Reddel,R. (2002) Telomere maintenance and cancer—look, no telomerase. *Nature Rev. Cancer*, **2**, 879–884.
- Lundblad,V. (2002) Telomere maintenance without telomerase. *Oncogene*, **21**, 522–531.
- Kass-Eisler,A. and Greider,C. (2000) Recombination in telomere-length maintenance. *Trends Biochem. Sci.*, **25**, 200–204.
- Garvik,B., Carson,M. and Hartwell,L. (1995) Single-stranded DNA arising at telomeres in *cdc13* mutants may constitute a specific signal for the RAD9 checkpoint. *Mol. Cell. Biol.*, **15**, 6128–6138.
- Maringle,L. and Lydall,D. (2002) EXO1-dependent single-stranded DNA at telomeres activates subsets of DNA damage and spindle checkpoint pathways in budding yeast *yku70Delta* mutants. *Genes Dev.*, **16**, 1919–1933.
- Yang,Q., Zheng,Y. and Harris,C. (2005) POT1 and TRF2 cooperate to maintain telomeric integrity. *Mol. Cell. Biol.*, **25**, 1070–1080.
- Baumann,P. and Cech,T.R. (2001) Pot1, the putative telomere end-binding protein in fission yeast and humans. *Science*, **292**, 1171–1175.
- Bertuch,A. and Lundblad,V. (2003) Which end: dissecting Ku's function at telomeres and double-strand breaks. *Genes Dev.*, **17**, 2347–2350.
- Fisher,T. and Zakian,V. (2005) Ku: A multifunctional protein involved in telomere maintenance. *DNA Repair*, **4**, 1215–1226.
- Gravel,S., Larrivee,M., Labrecque,P. and Wellinger,R.J. (1998) Yeast Ku as a regulator of chromosomal DNA end structure. *Science*, **280**, 741–744.
- Polotnianka,R.M., Li,J. and Lustig,A.J. (1998) The yeast Ku heterodimer is essential for protection of the telomere against nucleolytic and recombinational activities. *Curr. Biol.*, **8**, 831–834.
- Chan,S. and Blackburn,E. (2003) Telomerase and ATM/Tel1p protect telomeres from nonhomologous end joining. *Mol. Cell*, **11**, 1379–1387.
- Kim,M., Xu,L. and Blackburn,E. (2003) Catalytically active human telomerase mutants with allele-specific biological properties. *Exp. Cell Res.*, **288**, 277–287.
- McEachern,M.J. and Hicks,J.B. (1993) Unusually large telomeric repeats in the yeast *Candida albicans*. *Mol. Cell. Biol.*, **13**, 551–560.
- Singh,S.M., Steinberg-Neifach,O., Mian,I.S. and Lue,N.F. (2002) Analysis of telomerase in *Candida albicans*: potential role in telomere end protection. *Eukaryot Cell*, **1**, 967–977.
- Wilson,R.B., Davis,D. and Mitchell,A.P. (1999) Rapid hypothesis testing with *Candida albicans* through gene disruption with short homology regions. *J. Bacteriol.*, **181**, 1868–1874.
- Fonzi,W. and Irwin,M. (1993) Isogenic strain construction and gene mapping in *Candida albicans*. *Genetics*, **134**, 717–728.
- Hoffman,C. and Winston,F. (1987) A ten-minute DNA preparation from yeast efficiently releases autonomous plasmids for transformation of *Escherichia coli*. *Gene*, **57**, 267–272.
- Dionne,I. and Wellinger,R.J. (1996) Cell cycle-regulated generation of single-stranded G-rich DNA in the absence of telomerase. *Proc. Natl Acad. Sci. USA*, **93**, 13902–13907.
- Cimino-Reale,G., Pascale,E., Battiloro,E., Starace,G., Verna,R. and D'Ambrosio,E. (2001) The length of telomeric G-rich strand 3'-overhang measured by oligonucleotide ligation assay. *Nucleic Acids Res.*, **29**, E35.
- Stewart,S., Ben-Porath,I., Carey,V., O'Connor,B., Hahn,W. and Weinberg,R. (2003) Erosion of the telomeric single-strand overhang at replicative senescence. *Nature Genet.*, **33**, 492–496.
- Enloe,B., Diamond,A. and Mitchell,A. (2000) A single-transformation gene function test in diploid *Candida albicans*. *J. Bacteriol.*, **182**, 5730–5736.
- Lundblad,V. and Blackburn,E.H. (1993) An alternative pathway for yeast telomere maintenance rescues *est1*-senescence. *Cell*, **73**, 347–360.
- Teng,S., Chang,J., McCowan,B. and Zakian,V. (2000) Telomerase-independent lengthening of yeast telomeres occurs by an abrupt Rad50p-dependent, Rif-inhibited recombinational process. *Mol. Cell*, **6**, 947–952.
- Teng,S. and Zakian,V. (1999) Telomere-telomere recombination is an efficient bypass pathway for telomere maintenance in *Saccharomyces cerevisiae*. *Mol. Cell. Biol.*, **19**, 8083–8093.
- McEachern,M.J. and Blackburn,E.H. (1996) Cap-prevented recombination between terminal telomeric repeat arrays (telomere CPR) maintains telomeres in *Kluyveromyces lactis* lacking telomerase. *Genes Dev.*, **10**, 1822–1834.
- Topcu,Z., Nickles,K., Davis,C. and McEachern,M. (2005) Abrupt disruption of capping and a single source for recombinationally elongated telomeres in *Kluyveromyces lactis*. *Proc. Natl Acad. Sci. USA*, **102**, 3348–3353.

45. Lendvay,T.S., Morris,D.K., Sah,J., Balasubramanian,B. and Lundblad,V. (1996) Senescence mutants of *Saccharomyces cerevisiae* with a defect in telomere replication identify three additional *EST* genes. *Genetics*, **144**, 1399–1412.
46. McEachern,M. and Iyer,S. (2001) Short telomeres in yeast are highly recombinogenic. *Mol. Cell*, **7**, 695–704.
47. Beernink,H., Miller,K., Deshpande,A., Bucher,P. and Cooper,J. (2003) Telomere maintenance in fission yeast requires an est1 ortholog. *Curr. Biol.*, **13**, 575–580.
48. Reichenbach,P., Hoss,M., Azzalin,C., Nabholz,M., Bucher,P. and Lingner,J. (2003) A human homolog of yeast est1 associates with telomerase and uncaps chromosome ends when overexpressed. *Curr. Biol.*, **13**, 568–574.
49. Ciudad,T., Andaluz,E., Steinberg-Neifach,O., Lue,N., Gow,N., Calderone,R. and Larriba,G. (2004) Homologous recombination in *Candida albicans*: role of CaRad52p in DNA repair, integration of linear DNA fragments and telomere length. *Mol. Microbiol.*, **53**, 1177–1194.
50. Hackett,J. and Greider,C. (2003) End resection initiates genomic instability in the absence of telomerase. *Mol. Cell. Biol.*, **23**, 8450–8461.
51. Bertuch,A. and Lundblad,V. (2004) EXO1 contributes to telomere maintenance in both telomerase-proficient and telomerase-deficient *Saccharomyces cerevisiae*. *Genetics*, **166**, 1651–1659.
52. Fisher,T., Taggart,A. and Zakian,V. (2004) Cell cycle-dependent regulation of yeast telomerase by Ku. *Nature Struct. Mol. Biol.*, **11**, 1198–1205.
53. Stellwagen,A., Haimberger,Z., Veatch,J. and Gottschling,D. (2003) Ku interacts with telomerase RNA to promote telomere addition at native and broken chromosome ends. *Genes Dev.*, **17**, 2384–2395.
54. Smith,C., Smith,D., De,R.J. and Blackburn,E. (2003) Telomeric protein distributions and remodeling through the cell cycle in *Saccharomyces cerevisiae*. *Mol. Biol. Cell*, **14**, 556–570.
55. Cimino-Reale,G., Pascale,E., Alvino,E., Starace,G. and D'Ambrosio,E. (2003) Long telomeric C-rich 5'-tails in human replicating cells. *J. Biol. Chem.*, **278**, 2136–2140.